

Copper Complexes of Nitrogen-Anchored Tripodal N-Heterocyclic Carbene Ligands

Xile Hu, Ingrid Castro-Rodriguez, and Karsten Meyer*

Contribution from the Department of Chemistry and Biochemistry, Mail Code 0358,
University of California, San Diego, 9500 Gilman Drive, La Jolla, California 92093-0358

Received June 24, 2003; E-mail: kmeyer@ucsd.edu

Abstract: Incorporation of a nitrogen functionality into a tripodal N-heterocyclic carbene ligand system affords the first N-anchored tetradentate tris-carbene ligands TIMEN^R (R = Me (**5a**), *t*-Bu (**5b**), Bz (**5c**)). Treatment of the methyl derivatized [H₃TIMEN^{Me}](PF₆)₃ imidazolium salt (**5a**) with silver oxide yields the silver complex [(TIMEN^{Me})₂Ag₃](PF₆)₃ (**9**), which, in a ligand transfer reaction, reacts with copper(I) bromide to give the trinuclear copper(I) complex [(TIMEN^{Me})₂Cu₃](PF₆)₃ (**10**). Deprotonation of the *tert*-butyl and benzyl derivatives [H₃TIMEN^{*t*-Bu}](PF₆)₃ and [H₃TIMEN^{Bz}](PF₆)₃ yields the free tris-carbenes TIMEN^{*t*-Bu} (**5b**) and TIMEN^{Bz} (**5c**), which react readily with copper(I) salts to give mononuclear complexes [(TIMEN^{*t*-Bu})Cu](PF₆) (**11b**) and [(TIMEN^{Bz})Cu]Br (**11c**). The solid-state structures of **10**, **11b**, and **11c** were determined by single-crystal X-ray diffraction. While the TIMEN^{Me} ligand yields trinuclear complex **10**, with both T-shaped three-coordinate and linear two-coordinate copper(I) centers, the TIMEN^{*t*-Bu} and TIMEN^{Bz} ligands induce mononuclear complexes **11b** and **11c**, rendering the cuprous ion in a trigonal planar ligand environment of three carbenoid carbon centers and an additional, weak axial nitrogen interaction. Complexes **11b** and **11c** exhibit reversible one-electron redox events at half-wave potentials of 110 and −100 mV vs Fc/Fc⁺, respectively, indicating sufficient electronic and structural flexibility of both TIMEN^R ligands (R = *t*-Bu, Bz) to stabilize copper(I) and copper(II) oxidation states. Accordingly, a copper(II) NHC complex, [(TIMEN^{Bz})-Cu](OTf)₂ (**12**), was synthesized. Paramagnetic complex **12** was characterized by elemental analysis, EPR spectroscopy, and SQUID magnetization measurements.

Introduction

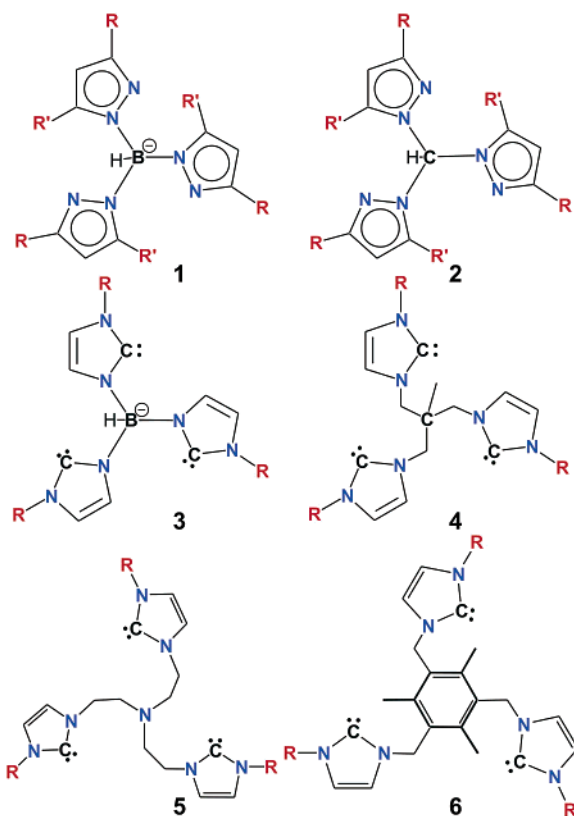
In recent years, tripodal ligand systems have increasingly gained importance in the field of transition metal coordination chemistry.^{1,2} Among those, derivatives of hydrotris(pyrazolyl)-borates (**1**) and their neutral carbon-anchored analogues, tris-(pyrazolyl)methane (**2**), are a unique class of ligands (Chart 1).^{3–5} Metal complexes supported by these tripodal donor ligands have been used extensively to promote catalytic transformations, such as C–H activation,⁶ C–C,⁷ C–O,⁸ and C–N⁹ bond formation, and serve as structural mimics of metal-containing enzymes.¹⁰

Substitution of the three pyrazolyl units in **1** with N-derivatized imidazole rings results in the N-heterocyclic carbene (NHC) analogues, hydrotris(3-alkylimidazol-2-ylidene)borate

(alkyl = Me, Et), **3**.^{11,12} Recent advances in the chemistry of NHC ligands^{13–20} have pushed these phosphine alternatives to the forefront of catalyst design, and numerous transition metal complexes bearing NHC ligands have been synthesized.^{15–17} However, known derivatives of boron-anchored carbene tripod **3** form coordinatively fully saturated, octahedral hexakis-carbene complexes such as the bis(triscarbene)iron complex [(**3**)₂Fe].¹¹ Consequently, ligand substitution reactions and redox events associated with small molecule and organic functional group activation have not been observed.^{11,12,21} The only other known tripodal tris-carbene ligand, 1,3,5-{tris(3-*tert*-butylimidazol-2-ylidene)methyl}-2,4,6-trimethylbenzene²² (**6**), has an exception-

- (1) Cummins, C. C.; Lee, J.; Schrock, R. R.; Davis, W. D. *Angew. Chem., Int. Ed. Engl.* **1992**, *31*, 1501–1503.
- (2) Brown, S. D.; Betley, T. A.; Peters, J. C. *J. Am. Chem. Soc.* **2003**, *125*, 322–323.
- (3) Trofimenko, S. *Scorpionates, The Coordination Chemistry of Polypyrazolylborate Ligands*; Imperial College Press: London, 1999.
- (4) Trofimenko, S. *Prog. Inorg. Chem.* **1986**, *34*, 115–210.
- (5) Trofimenko, S. *Chem. Rev.* **1993**, *93*, 943–980.
- (6) Slugovc, C.; Padilla-Martinez, I.; Sirol, S.; Carmona, E. *Coord. Chem. Rev.* **2001**, *213*, 129–157.
- (7) Diaz-Requejo, M. M.; Belderrain, T. R.; Trofimenko, S.; Perez, P. J. *J. Am. Chem. Soc.* **2001**, *123*, 3167–3168.
- (8) Diaz-Requejo, M. M.; Belderrain, T. R.; Perez, P. J. *Chem. Commun.* **2000**, 1853–1854.
- (9) Morilla, M. E.; Diaz-Requejo, M. M.; Belderrain, T. R.; Nicasio, M. C.; Trofimenko, S.; Perez, P. J. *Chem. Commun.* **2002**, 2998–2999.
- (10) Parkin, G. *Chem. Commun.* **2000**, 1971–1985.

- (11) Kernbach, U.; Ramm, M.; Luger, P.; Fehlhammer, W. P. *Angew. Chem., Int. Ed. Engl.* **1996**, *35*, 310–312.
- (12) Frankel, R.; Birg, C.; Kernbach, U.; Haberer, T.; Noth, H.; Fehlhammer, W. P. *Angew. Chem., Int. Ed.* **2001**, *40*, 1907–1910.
- (13) Arduengo, A. J.; Harlow, R. L.; Kline, M. *J. Am. Chem. Soc.* **1991**, *113*, 361–363.
- (14) Arduengo, A. J. *Acc. Chem. Res.* **1999**, *32*, 913–921.
- (15) Bourissou, D.; Guerret, O.; Gabbai, F. P.; Bertrand, G. *Chem. Rev.* **2000**, *100*, 39–91.
- (16) Herrmann, W. A.; Kocher, C. *Angew. Chem., Int. Ed. Engl.* **1997**, *36*, 2163–2187.
- (17) Herrmann, W. A. *Angew. Chem., Int. Ed.* **2002**, *41*, 1291–1309.
- (18) Scholl, M.; Ding, S.; Lee, C. W.; Grubbs, R. H. *Org. Lett.* **1999**, *1*, 953–956.
- (19) Huang, J. K.; Stevens, E. D.; Nolan, S. P.; Petersen, J. L. *J. Am. Chem. Soc.* **1999**, *121*, 2674–2678.
- (20) Peris, E.; Loch, J. A.; Mata, J.; Crabtree, R. H. *Chem. Commun.* **2001**, 201–202.
- (21) Frankel, R.; Kernbach, U.; Bakola-Christianopoulou, M.; Plaia, U.; Suter, M.; Ponikvar, W.; Noth, H.; Moinet, C.; Fehlhammer, W. P. *J. Organomet. Chem.* **2001**, *617*, 530–545.

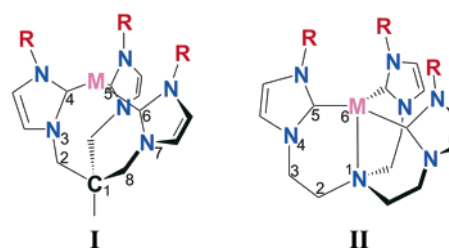
Chart 1. Structural Representatives for Tripodal Polypyrazolyl and Polycarbene Ligands

ally big cavity and coordinates exclusively to large metal ions such as the monovalent thallium(I) ion.²³ Therefore, the development of potent tris-carbene ligand systems for transition metal coordination and subsequent application in homogeneous catalysis and small molecule activation are current efforts in our laboratory.

In this context, we recently reported the synthesis and coordination chemistry of tris-carbene ligand system **4**, 1,1,1-[tris-(3-alkylimidazol-2-ylidene)methyl]ethane (TIME^R, R = Me (**4a**), *t*-Bu (**4b**)), reminiscent of ligands of type 2.^{24,25} With group 11 metal ions, the methyl derivative TIME^{Me} exclusively forms isostructural complexes of the general type [(TIME^{Me})₂M₃]³⁺ (M = Cu (**7**), Ag, Au), comprising two-coordinate metal centers with a linear binding mode (Scheme 1, A).²⁴

The sterically more demanding *tert*-butyl derivatized ligand system TIME^{*t*-Bu} (**4b**) induces the formation of an interesting dinuclear copper(I) bis-carbenealkenyl complex, [(TIME^{*t*-Bu})₂Cu₂]²⁺ (**8**, Scheme 1, B).²⁵

These findings demonstrate the versatility of type **4** ligands; yet, in our hands, mononuclear metal complexes of these carbon-anchored chelators remained elusive. Similar observations were made by others for the analogous tris-pyrazolyl ligand system **4**.²⁶ It was reported that the ligand 1,1,1-[tris(pyrazol-1-yl)-methyl]ethane tends to act as a bidentate chelator; thus, simple

Chart 2. Structural Models for Metal Complexes of Tripodal Neopentane C- and N-Anchored Carbene Chelators

η^3 complexes could not be isolated.²⁶ Examination of the backbones of the neopentane-based, carbon-anchored tripodal ligands reveals possible reasons for the lack of 1:1 complex formation with these chelators. A hypothetical η^3 complex of chelator **4** would contain three eight-membered rings (**I**, Chart 2) with much lower stability than the more commonly observed five-, six-, or seven-membered rings formed, for instance, by polypyrazolylborate⁴ or polyphosphine²⁷ ligands.

Consequently, methyl derivative **4a** yields highly *D*₃-symmetrical trinuclear complexes and has no tendency for metal-lacycle formation. Increased steric bulk at the imidazole N3-position of *tert*-butyl derivative **4b** effectively prevents the formation of trinuclear complexes of type **7** (Scheme 1). However, because formation of three eight-membered rings is entropically unfavorable, mononuclear complex formation still cannot be observed. Instead, a dinuclear 2:2 complex **8** with only one such unusual eight-membered ring per ligand molecule was isolated. To overcome these inherent deficits of ligands of type **4**, we sought to incorporate a coordinating atom at the anchoring position of the carbene tripod, engendering ligands that favor 1:1 metal complexation by forming three stable six-membered rings (**II**, Chart 2). Accordingly, the nitrogen-anchored tris-carbene ligand system tris[2-(3-alkylimidazol-2-ylidene)ethyl]amine (TIMEN^R, R = Me, *t*-Bu, Bz) (**5**) and corresponding copper(I) and (II) complexes were synthesized.

Results and Discussion

Ligand Synthesis. The imidazolium precursors, tris-[2-(3-alkylmethylimidazolium-1-yl)ethyl]amine trichloride [H₃TIMEN^R]-Cl₃ (R = Me, *t*-Bu, and Bz), were prepared by quaternization of functionalized *N*-alkylimidazoles with tris-(2-chloroethyl)-amine. Treatment of [H₃TIMEN^R]-Cl₃ in methanol with ammonium hexafluorophosphate effected complete substitution of chloride and formation of [H₃TIMEN^R](PF₆)₃ (**H₃5a**, R = Me; **H₃5b**, R = *t*-Bu; **H₃5c**, R = Bz). Highest yields for all quaternization reactions were achieved by heating the neat reactants at 150 °C for 2 days. Deprotonation of **H₃5a** with strong base fails to produce free carbene ligand **5a**; however, a copper(I) complex of this ligand is accessible via a transmetalation route²⁸ employing the corresponding silver complex of this ligand (vide infra). Deprotonation of **H₃5b** and **H₃5c** with potassium *tert*-butoxide yields free tris-carbene ligands **5b** and **5c**, which can be isolated and stored under nitrogen for further transformation. Ligands **5b** and **5c** were characterized by ¹H and ¹³C NMR spectroscopy. The characteristic ¹³C signals for the deprotonated carbene carbon atoms were found at δ = 213.6 (**5b**) and 211.8 ppm (**5c**).

(22) Dias, H. V. R.; Jin, W. C. *Tetrahedron Lett.* **1994**, 35, 1365–1366.

(23) Nakai, H.; Tang, Y. J.; Gantzel, P.; Meyer, K. *Chem. Commun.* **2003**, 24–25.

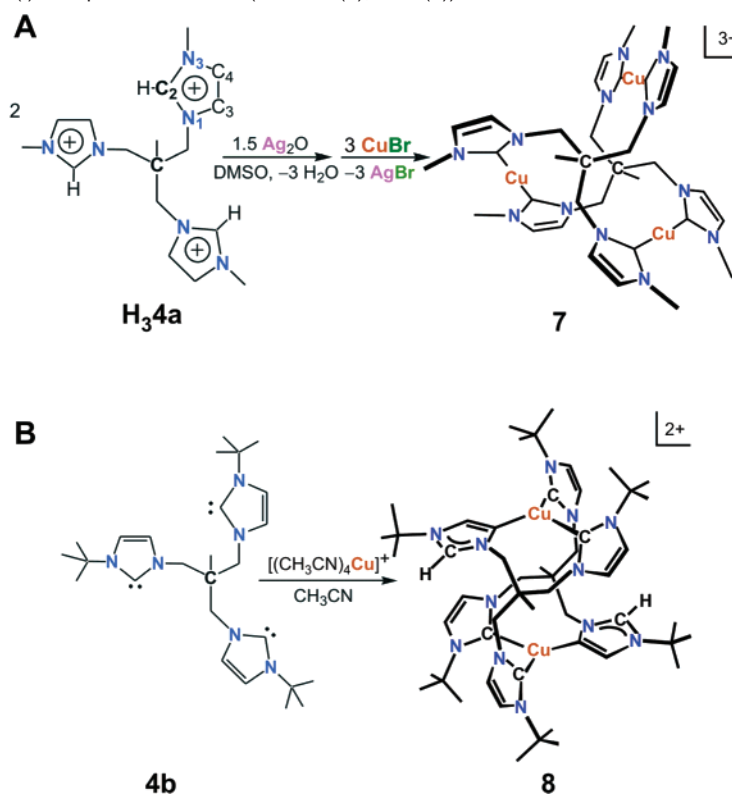
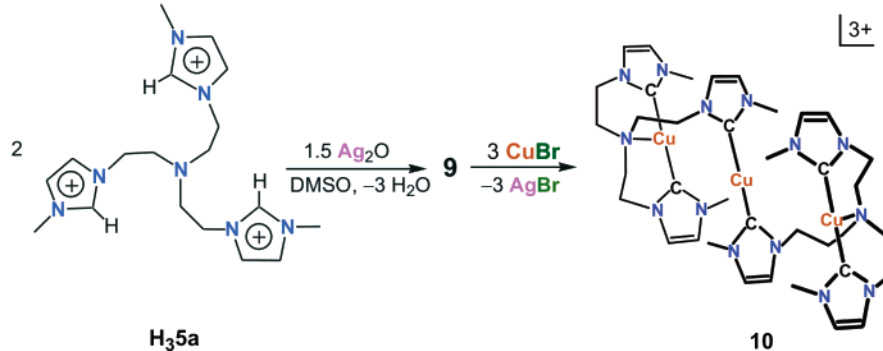
(24) Hu, X.; Tang, Y.; Gantzel, P.; Meyer, K. *Organometallics* **2003**, 22, 612–614.

(25) Hu, X.; Castro-Rodriguez, I.; Meyer, K. *Organometallics* **2003**, 22, 3016–3018.

(26) Jacobi, A.; Huttner, G.; Winterhalter, U.; Cunsakis, S. *Eur. J. Inorg. Chem.* **1998**, 675–692.

(27) Mayer, H. A.; Kaska, W. C. *Chem. Rev.* **1994**, 94, 1239–1272.

(28) Wang, H. M. J.; Lin, I. J. B. *Organometallics* **1998**, 17, 972–975.

Scheme 1. Synthesis of Copper(I) Complexes of TIMER^R (R = Me (**7**), *t*-Bu (**8**))**Scheme 2.** Synthesis of Trinuclear Complex [(TIMEN^{Me})₂Cu₃]³⁺ (**10**)

Synthesis and Characterization of Trinuclear [(TIMEN^{Me})₂Cu₃](PF₆)₃ (10**).** Reaction of the methyl derivatized [H₃TIMEN^{Me}](PF₆)₃ imidazolium salt **H₃5a** with Ag₂O in DMSO at 75 °C yields a silver complex, [(TIMEN^{Me})₂Ag₃](PF₆)₃ (**9**).²⁹ Treatment of trinuclear **9** with 3 equiv of CuBr in acetonitrile leads to formation of a copper(I) complex [(TIMEN^{Me})₂Cu₃](PF₆)₃·2.5 CH₃CN (**10**) (Scheme 2). The solid-state structure of **10** reveals a trinuclear complex with two distinctly different coordination geometries of the cuprous ions (Figure 1).

Each TIMEN^{Me} ligand exhibits coordination to two different Cu(I) centers in nearly centro-symmetric fashion without a crystallographic inversion center. Two of the three pendant carbene ligators and the anchoring nitrogen atom of one ligand molecule coordinate to one Cu(I) ion to give a T-shaped ligand environment. The third carbene, together with that of the second ligand, coordinates to a central Cu(I) ion in linear fashion. The latter feature is reminiscent of the linear C–M–C fragments in **7**.

The Cu–C distances in **10** range between 1.889 and 1.902 Å for the three-coordinate copper ions and 1.908–1.911 Å for the two-coordinate copper ions. These values compare well to those found for other reported Cu–NHC complexes.^{30,31} The average Cu–N distance of 2.365 Å for both three-coordinate copper ions is significantly longer than values typically found for tris(2-aminoethyl)amine-based copper(I) complexes of ~2.2 Å.^{32,33} This weak interaction of the nitrogen anchor with the copper ions is also reflected in the crystallographically determined, near linear C_{carbene}–Cu–C_{carbene} angles of ~170° for the three-coordinate cuprous and ~180° for the two-coordinate Cu(I) ions. As a result of this weak but significant Cu–N-(anchor) interaction, each TIMEN^{Me} ligand forms two of the expected three six-membered rings with one copper ion. Overall,

(29) Although crystals of **9** suitable for X-ray diffraction study were not obtained, we suggest the isostructural geometry for **9** and **7** on the basis of the similarity of characteristic features in the ¹H and ¹³C NMR spectra.

(30) Arnold, P. L.; Scarisbrick, A. C.; Blake, A. J.; Wilson, C. *Chem. Commun.* **2001**, 2340–2341.

(31) Tulloch, A. A. D.; Danopoulos, A. A.; Kleinhenz, S.; Light, M. E.; Hursthouse, M. B.; Eastham, G. *Organometallics* **2001**, *20*, 2027–2031.

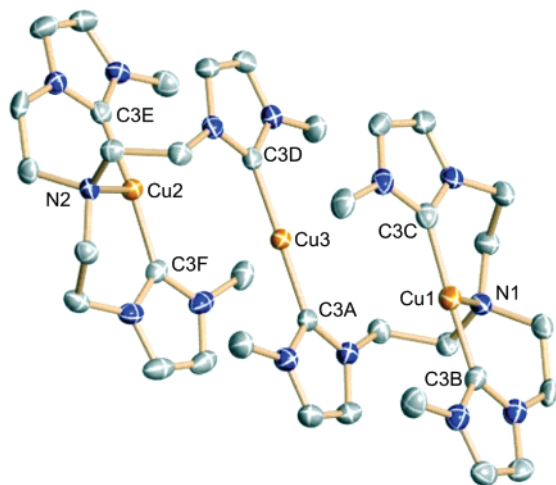
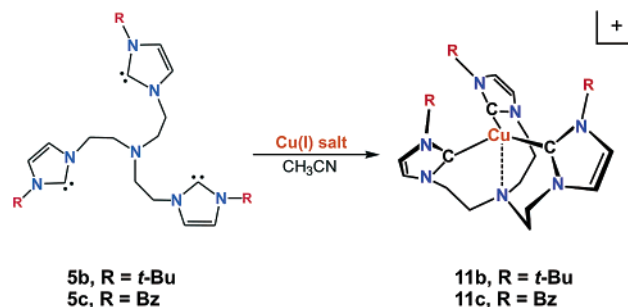


Figure 1. Solid-state molecular structure of complex $[(\text{TIMEN}^{\text{Me}})_2\text{Cu}_3]-(\text{PF}_6)_3 \cdot 2.5\text{CH}_3\text{CN}$ (**10**). Hydrogen atoms, anions, and solvent molecules are omitted for clarity; thermal ellipsoids are at 50% probability. Selected bond lengths (Å) and angles (deg): Cu(1)–C(3B) 1.901(4), Cu(1)–C(3C) 1.894(5), Cu(1)–N(1) 2.365(3), Cu(2)–C(3E) 1.892(4), Cu(2)–C(3F) 1.891(4), Cu(2)–N(2) 2.371(3), Cu(3)–C(3A) 1.909(4), Cu(3)–C(3D) 1.910(4), C(3B)–Cu(1)–C(3C) 172.54(19), C(3E)–Cu(2)–C(3F) 166.50(17), C(3A)–Cu(3)–C(3D) 178.74(17).

Scheme 3. Synthesis of Mononuclear Complexes $[(\text{TIMEN}^{\text{R}})\text{Cu}]^+$ ($\text{R} = t\text{-Bu}$ (**11b**), Bz (**11c**))



however, formation of the unique structure of **10** was unexpected because no obvious steric hindrance appears to be preventing a 1:1 metal complex formation of the methyl-substituted derivative. We therefore conclude that formation of complex **10** is kinetically controlled. This is likely due to the presence of excess Cu(I) ions in solution resulting from the transmetalation reaction of trinuclear **9** with 3 equiv of Cu(I) salt to eliminate 3 equiv of AgBr.

Synthesis and Characterization of Mononuclear $[(\text{TIMEN}^{\text{R}})\text{Cu}]^+$ (11b**, $\text{R} = t\text{-Bu}$; **11c**, $\text{R} = \text{Bz}$).** Reaction of free carbene $\text{TIMEN}^{t\text{-Bu}}$ **5b** with 1 equiv of $[(\text{CH}_3\text{CN})_4\text{Cu}](\text{PF}_6)$ in acetonitrile affords the mononuclear 1:1 copper complex **11b** as an off-white powder in high yields (~60%) (Scheme 3).

The solid-state structure of mononuclear tris-carbene copper complex **11b** was determined by single-crystal X-ray diffraction analysis (Figure 2). The tripodal carbene ligand **5b** coordinates to the copper ion via the three carbenoid carbons in the predicted tridentate fashion. The long Cu–N distance of 2.567(3) Å and a displacement toward the N-anchor of only 0.02 Å out of the idealized trigonal plane suggest that the interaction of the anchoring nitrogen atom with the copper ion is electronically

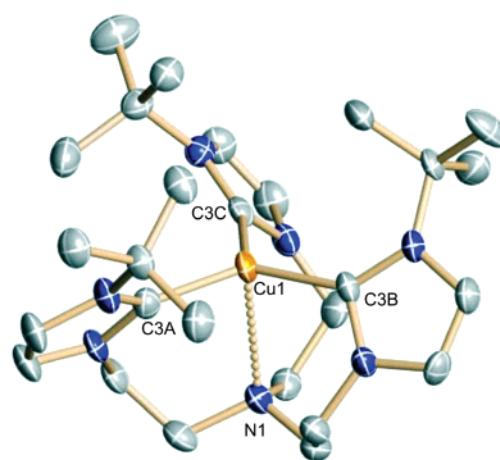


Figure 2. Solid-state molecular structure of complex $[(\text{TIMEN}^{t\text{-Bu}})\text{Cu}](\text{PF}_6)$ (**11b**). Hydrogen atoms and anions are omitted for clarity; thermal ellipsoids are at 50% probability. Selected bond lengths (Å) and angles (deg): Cu(1)–C(3A) 1.976(3), Cu(1)–C(3B) 1.987(3), Cu(1)–C(3C) 1.993(3), Cu(1)–N(1) 2.567(3), C(3A)–Cu(1)–C(3B) 120.03(12), C(3A)–Cu(1)–C(3C) 117.96(12), C(3B)–Cu(1)–C(3C) 121.98(12).

nonsignificant. This interaction, however, does stabilize compound **11b** structurally, as it leads to the formation of three six-membered metallacycles (Scheme 3). This copper(I) complex represents the first example of a 1:1 transition metal complex of a polydentate tris-carbene ligand. The average Cu–C_{carbene} distance of 1.985 Å is slightly longer than that of complex **10**, consistent with the presence of three sterically demanding *tert*-butyl groups at the N3 positions of the imidazole rings. The copper(I) ion is located in an ideal trigonal planar ligand environment with an average C–Cu–C angle of 119.99°.

The NMR spectra of **11b** are consistent with the solid-state structure determined by X-ray crystallography. In the ^1H spectrum, the six C4/C5 protons of the imidazole rings give rise to two sets of doublets with equal intensity at $\delta = 7.19$ and 6.92 ppm, and the three *tert*-butyl groups result in only one intense signal at $\delta = 1.52$ ppm, indicative of a C_3 symmetrical molecule in solution. The 12 protons of the ethylene backbones of **11b** give rise to four doublets of doublets with equal intensity and are observed at $\delta = 3.67$, 3.43, 2.90, and 2.34 ppm, respectively. The ^{13}C spectrum exhibits only one signal for the carbenoid carbon at $\delta = 187$ ppm.

The redox behavior of the novel mononuclear compound was examined by electrochemical methods. The cyclic voltammogram of a solution of **11b** in acetonitrile exhibits a reversible one-electron oxidation at a potential of +110 mV vs Fc/Fc⁺ (Figure 3). The reversibility for the Cu(I)/Cu(II) couple was confirmed by measuring the ratios of $I_{\text{ox}}/I_{\text{red}}$ as a function of scan rates and peak separation. For all scan rates, values for $I_{\text{ox}}/I_{\text{red}}$ were determined to be approximately 1. The peak separation, $|E_{\text{ox}} - E_{\text{red}}|$ at 300 mV s^{−1}, was calculated to be 66 mV (see Figure S1, Supporting Information). This reversible redox behavior indicates that the $\text{TIMEN}^{t\text{-Bu}}$ ligand has sufficient structural and electronic flexibility to accommodate the copper ion in both the Cu(I) and the Cu(II) oxidation states.

A space-filling model of complex **11b** (Figure 4) suggests that the electron-rich cuprous ion in this complex is well shielded by the three sterically encumbering *tert*-butyl groups. To facilitate enhanced reactivity at the electron-rich metal center, a Cu(I) complex with the sterically less demanding benzyl-substituted

(32) Becker, M.; Heinemann, F. W.; Schindler, S. *Chem.-Eur. J.* **1999**, *5*, 3124–3129.

(33) Raab, V.; Kipke, J.; Burghaus, O.; Sundermeyer, J. *Inorg. Chem.* **2001**, *40*, 6964–6971.

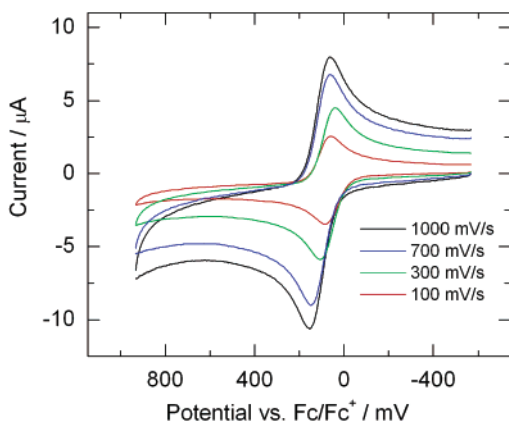


Figure 3. Cyclic voltammogram of [(TIMEN^{t-Bu})Cu](PF₆) (**11b**) recorded in acetonitrile solution containing 0.1 M [N(*n*-Bu)₄](ClO₄) as electrolyte.

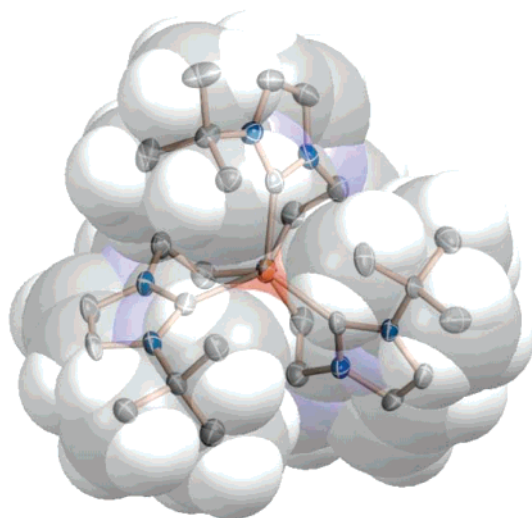


Figure 4. Space-filling model for [(TIMEN^{t-Bu})Cu](PF₆) (**11b**).

TIMEN^{Bz} ligand, [(TIMEN^{Bz})Cu]Br (**11c**), was synthesized by reacting free carbene **5c** with copper(I) bromide (Scheme 3).

The molecular structure of compound **11c** was determined by single-crystal X-ray diffraction study. Complex **11c** crystallizes with three independent molecules in the asymmetric unit. The solid-state structure of one of the three independent molecules is depicted in Figure 5. The average Cu–C bond length of 1.958 Å is slightly shorter than that of complex **11b**, consistent with reduced steric bulk of the benzyl substituents. The average Cu(I)–N(amine) interaction of 2.415 Å in **11c**, however, is considerably stronger than that of 2.567(3) Å in **11b**. The space-filling model (Figure 6) shows the expected open cavity at the Cu(I) ion exposed by the three less protective benzyl groups. The cyclic voltammogram of complex **11c** exhibits a reversible one-electron oxidation at –100 mV vs Fc/Fc⁺, 210 mV lower than that of **11b** (Figure S2, Supporting Information). The benzyl-substituted ligand **5c** thus seems to be significantly more flexible with regard to structural changes upon oxidation.

Synthesis and Characterization of [(TIMEN^{Bz})Cu](OTf)₂ (12**).** The one-electron oxidized Cu(II) complex, [(TIMEN^{Bz})Cu](OTf)₂ (**12**), was synthesized via two different, independent routes. The complex could be obtained by either oxidizing **11c** with silver(I) triflate or, alternatively, by reacting ligand **5c** with copper(II) triflate. Reaction of **5c** with other copper(II) salts,

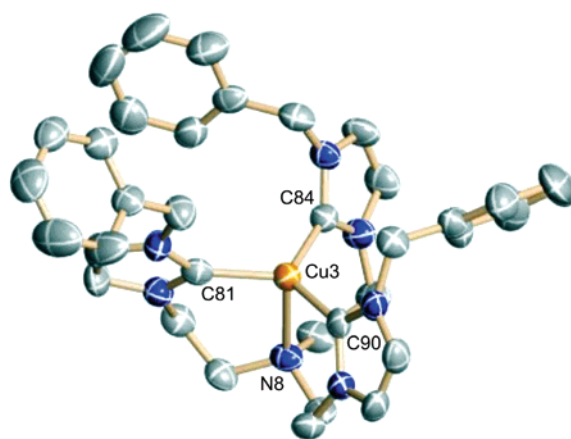


Figure 5. Solid-state molecular structure of complex [(TIMEN^{Bz})Cu](Br) (**11c**). Mononuclear **11c** crystallizes with three independent molecules per unit cell, in which bond lengths and angles vary slightly. Hydrogen atoms, anions, and the remaining two independent molecules are omitted for clarity; thermal ellipsoids are at 50% probability. Selected bond lengths (Å) and angles (deg): Cu–C_{carbene} (av.) 1.949, 1.961, and 1.965, Cu–N_{amine} 2.365(4), 2.399(4), and 2.482(4), N–C_{carbene}–N (av.) 103.10, 102.78, and 102.61, C–Cu–C (av.) 119.91, 119.68, and 119.56.

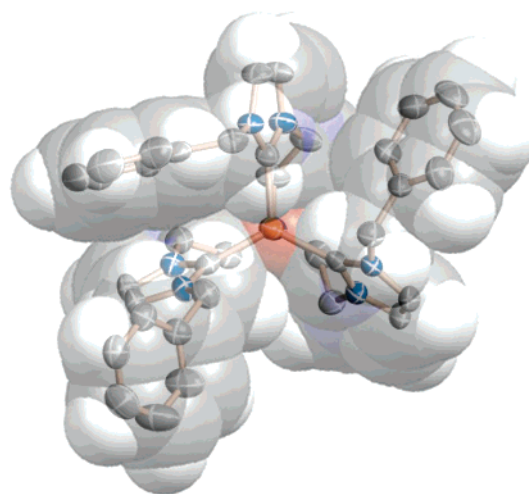


Figure 6. Space-filling model for [(TIMEN^{Bz})Cu](Br) (**11c**).

for instance, copper(II) bromide, leads to formation of unidentified diamagnetic materials.

Paramagnetic compound **12** was characterized by elemental analysis, low-temperature X-band EPR spectroscopy, and variable temperature SQUID magnetization measurements. The X-band EPR spectrum of **12**, recorded in frozen acetonitrile/toluene solution at 8 K, exhibits a rhombic signal (Figure 7, top). The signal can be simulated to high accuracy with $g_1 = 2.005$, $g_2 = 2.060$, and $g_3 = 2.275$, and a copper hyperfine coupling constant $A_3(^{63}\text{Cu}, I = 3/2, 100\%)$ of $132 \times 10^{-4} \text{ cm}^{-1}$ (397 MHz). Copper hyperfine interactions on g_1 and g_2 are not resolved. The EPR spectrum of **12** is consistent with a mononuclear copper(II) complex with one unpaired electron.

The solid-state magnetization measurement of solid samples of **12** confirms the copper(II) oxidation state of the complex. The temperature dependence of the magnetic moment was determined in the temperature range from 5 to 300 K (Figure 7, bottom). At room temperature, complex **12** exhibits a magnetic moment of $1.86 \mu_B$, which is in good agreement with the calculated value of $1.83 \mu_B$ obtained by applying the average g

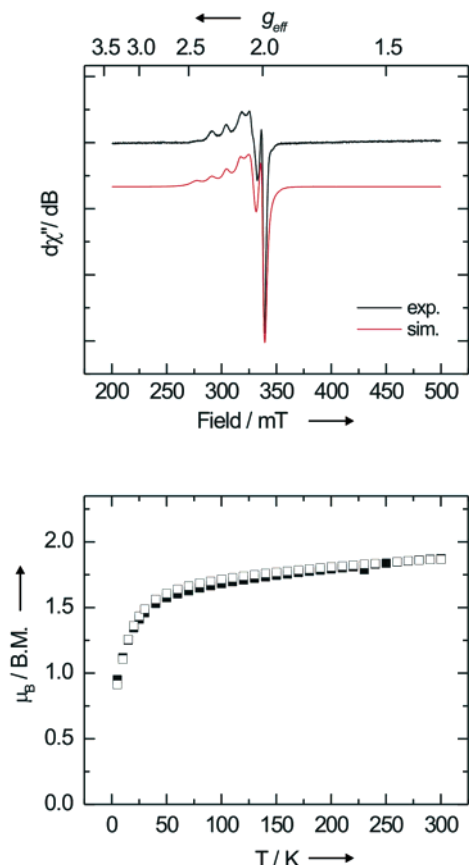


Figure 7. X-band EPR spectrum of **12** (top) recorded in frozen acetonitrile/toluene solution at 8 K. Experimental conditions: microwave frequency ν , 9.4666 GHz; power, 0.63 mW; modulation amplitude, 10 G. Simulated parameters: $g_1 = 2.005$ ($W_1 = 20.00$ G); $g_2 = 2.060$ ($W_2 = 55.00$ G); $g_3 = 2.275$ ($W_3 = 42.00$ G); $A_3 = 132 \times 10^{-4} \text{ cm}^{-1}$ (397.00 MHz). Plot of the effective magnetic moment, μ_{eff} , versus temperature from temperature-dependent SQUID magnetization measurements for two independently prepared samples of **12** (bottom).

value of 2.11 determined by EPR spectroscopy. The magnetic moment of 1.86 μ_B at room temperature decreases slightly to $\sim 1.71 \mu_B$ at 100 K, and then continues to decrease, reaching a minimum of 0.91 μ_B at 5 K. This observed temperature behavior indicates weak antiferromagnetic spin–spin coupling in the solid state.

The EPR spectroscopy and SQUID magnetization measurements suggest that the unpaired electron in complex **12** resides in the copper $3d(x^2 - y^2)$ orbital. The ground-state electronic structure of **12** was further elucidated with the aid of DFT calculations. Our DFT studies (BP86/TZP, ZORA, ADF 2003.01)^{34–36} on the model complex $[\text{TIMEN}^{\text{Me}}\text{Cu}]^{2+}$ indicate that the copper(II) ion in **12** retains the trigonal-planar ligand environment, with a weak axial Cu–N(amine) interaction ($d_{\text{calcd}} \text{ Cu–N} = 2.54 \text{ \AA}$) (Figure 8, top). The CuC_3 plane exhibits a Jahn–Teller distortion, rendering one C–Cu–C angle significantly larger (139.7°) than the other two (112.5° and 107.4°). A similar distortion is found in the copper–carbene bond distances. The Cu–C bond opposite to the largest C–Cu–C angle is significantly longer (1.965 \AA) than the other two Cu–C

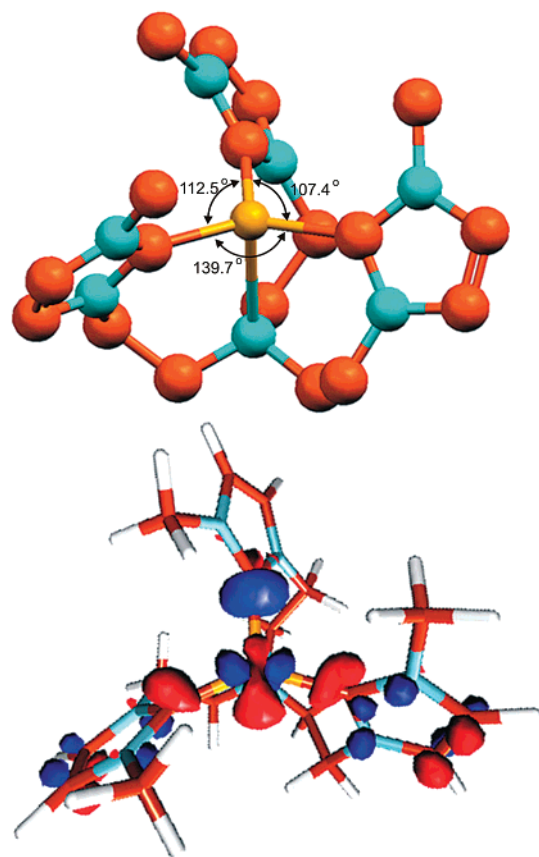


Figure 8. Geometry-optimized structure of model compound $[\text{TIMEN}^{\text{Me}}\text{Cu}]^{2+}$ (top) and singly occupied molecular orbital (SOMO) in the system of complex $[\text{TIMEN}^{\text{Me}}\text{Cu}]^{2+}$ (bottom).

bonds at 1.935 and 1.936 \AA , respectively. This distortion in the Cu–C₃ plane raises the energy of the metal d-orbital $d(x^2 - y^2)$ above $d(xy)$ and $d(z^2)$ and thus removes the degeneracy of the $d(x^2 - y^2)$ and $d(xy)$ orbitals. This departure from an idealized trigonal plane results in a $d(xz)^2d(yz)^2d(xy)^2-d(z^2)^2d(x^2 - y^2)^1$ ground-state electronic configuration for the geometry-optimized complex $[\text{TIMEN}^{\text{Me}}\text{Cu}]^{2+}$. The singly occupied molecular orbital (SOMO) is depicted in Figure 8, bottom. A full set of molecular orbitals is depicted in Figure S3, Supporting Information.

Conclusion

In summary, strikingly different Cu(I) complexes have been synthesized by employing three derivatives of the same tripodal, tris-carbene ligand system tris[2-(3-alkylimidazol-2-ylidene)-ethyl]amine (TIMEN^{R} , R = Me, *t*-Bu, Bz) (**5**). The methyl substituted ligand, TIMEN^{Me} (**5a**), yields, via a transmetalation route, the trinuclear complex $[(\text{TIMEN}^{\text{Me}})_2\text{Cu}_3]^{3+}$ (**10**). This complex contains one linear two-coordinate and two T-shaped three-coordinate copper(I) centers (Scheme 2). In contrast, the sterically more encumbering *tert*-butyl and benzyl derivatized free carbenes $\text{TIMEN}^{\text{t-Bu}}$ (**5b**) and TIMEN^{Bz} (**5c**) induce the formation of mononuclear complexes, $[(\text{TIMEN}^{\text{R}})\text{Cu}]^+$ (**11b**, R = *t*-Bu; **11c**, R = Bz) (Schemes 3). To the best of our knowledge, mononuclear complexes **11b** and **11c** represent the first examples of a 1:1 transition metal complex of a polydentate tris-carbene ligand. The trigonal planar carbene environment of the Cu(I) and Cu(II) metal centers in all mononuclear complexes presented herein is unprecedented in NHC coordina-

(34) Velde, G. T.; Bickelhaupt, F. M.; Baerends, E. J.; Guerra, C. F.; Van Gisbergen, S. J. A.; Snijders, J. G.; Ziegler, T. *J. Comput. Chem.* **2001**, *22*, 931–967.

(35) Perdew, J. P. *Phys. Rev. B* **1986**, *33*, 8822–8824.

(36) Becke, A. D. *Phys. Rev. A* **1988**, *38*, 3098–3100.

tion chemistry. The open coordination site at the electron-rich copper(I) center in **11c** likely enhances chemical transformations of various substrates. The reversible redox behavior of complex **11c** and successful synthesis of the one-electron oxidized Cu(II) species **12** support the prospect of versatile reactivity resulting from complexes of this ligand system. Complex **12** represents the first isolated and spectroscopically characterized copper(II) NHC complex to date. Further detailed investigations of the electronic structure of this paramagnetic copper–carbene complex will result in an enhanced understanding of the donor/acceptor abilities of NHC ligands. Continuing electronic structure and reactivity studies of copper(I/II) complexes **11c** and **12** are currently underway.

Experimental Section

Methods and Procedures. Manipulation of air-sensitive compounds was performed under a controlled dry nitrogen atmosphere using standard Schlenk techniques and inert-gas gloveboxes (MBraun Labmaster by M. Braun, Inc.). Solvents were purified using a two-column solid-state purification system (Glasscontour System, Joerg Meyer, Irvine, CA) and transferred to the glovebox without exposure to air. NMR solvents were obtained from Cambridge Isotope Laboratories, degassed, and stored over activated molecular sieves prior to use. All NMR spectra were recorded at room temperature (20 °C) in *d*₆-benzene, *d*₃-acetonitrile, and *d*₆-DMSO solutions on Varian spectrometers operating at 400/300 MHz (¹H NMR) and 100 MHz (¹³C NMR) and were referenced to residual solvent peaks unless otherwise noted (δ in ppm). Cyclic voltammetric measurements were performed on Bioanalytical Systems equipment (BAS, CV-50W) in acetonitrile solutions containing 0.1 M [N(*n*-Bu)₄](ClO₄) as electrolyte (working electrode, platinum; auxiliary electrode, platinum wire; reference electrode, platinum). Potentials are reported relative to the ferrocene/ferrocenium couple (Fc/Fc⁺). X-band EPR spectra of dilute complex solutions in a 1:1 mixture of acetonitrile and toluene were recorded on a Bruker Elexsys E500 spectrometer equipped with a helium flow cryostat (Oxford 900). The spectra were simulated using the W95EPR program.³⁷ Solid-state magnetization measurements of powdered samples were recorded on a SQUID magnetometer (Quantum Design) at 10 kOe between 5 and 300 K. Magnetic susceptibility data were corrected for background and underlying diamagnetic contributions (χ_{dia} = −515 × 10^{−6} cm³ mol^{−1}) using tabulated Pascal constants.³⁸ Data reproducibility was carefully checked in multiple individual measurements of independently synthesized samples. Elemental analyses were performed by Kolbe Microanalytical Laboratory (Muelheim a. d. Ruhr/Germany).

Starting Materials. *N*-tert-Butylimidazole,³⁹ tris(2-chloroethyl)amine,⁴⁰ and tetrakis(acetonitrile)copper(I) hexafluorophosphate⁴¹ were prepared according to literature procedures. *N*-Methylimidazole (Acros), *N*-benzylimidazole (Aldrich), silver oxide (Fischer), silver triflate (Strem), copper(I) bromide (Acros), copper(II) triflate (Strem), potassium *tert*-butoxide (Acros), ammonium hexafluorophosphate (Aldrich), and tetra(*n*-butyl)ammonium perchlorate (Aldrich) were obtained from commercial sources and used as received.

Synthesis. [H₃TIMEN^{Me}](PF₆)₃ (**H₃5a**). A 50 mL flask was charged with tris(2-chloroethyl)amine (4.1 g, 20 mmol) and *N*-methylimidazole (4.95 g, 60 mmol), and the mixture was heated to 150 °C for 2 days, during which a brown solid formed. The solid was filtered off and dissolved in 20 mL of methanol, and the filtered solution was evaporated to dryness to yield the crude product [H₃TIMEN^{Me}]Cl₃ (6.0 g, yield: 67%). The hygroscopic chloride salt was converted to the corresponding,

stable hexafluorophosphate salt, [H₃TIMEN^{Me}](PF₆)₃, by adding solid NH₄PF₆ (6.5 g, 40.6 mmol) to a solution of [H₃TIMEN^{Me}]Cl₃ (6.9 g, 13.3 mmol) in 20 mL of methanol. The white hexafluorophosphate salt precipitated immediately, and was collected by filtration, washed with small portions of cold methanol, and dried in a vacuum (8.5 g; yield: 82%).

¹H NMR (300 MHz, *d*₆-DMSO, 20 °C): δ = 8.94 (s, 3H), 7.67 (s, 3H), 7.58 (s, 3H), 4.19 (t, ³J(H,H) = 6.0 Hz, 6H), 3.84 (s, 9H), 2.95 ppm (t, ³J(H,H) = 6.0 Hz, 6H). ¹³C NMR (100 MHz, *d*₆-DMSO, 20 °C): δ = 136.7, 123.0, 122.3, 52.1, 45.9, 35.8 ppm. Anal. Calcd for C₁₈H₃₀F₁₈N₇P₃: C, 27.74; H, 3.88; N, 12.58. Found: C, 28.10; H, 3.92; N, 12.61.

[TIMEN^{*t*-Bu}](PF₆)₃ (**H₃5b**). A 50 mL flask was charged with tris(2-chloroethyl)amine (2.1 g, 10 mmol) and *N*-tert-butylimidazole (3.9 g, 31 mmol), and the mixture was heated to 150 °C for 3 days, during which a brown solid formed. The solid was filtered off and dissolved in 20 mL of methanol, and the filtered solution was evaporated to dryness to yield the crude product [H₃TIMEN^{*t*-Bu}]Cl₃ (5.6 g; yield: 97%). The hygroscopic chloride salt was converted to stable [H₃TIMEN^{*t*-Bu}](PF₆)₃ by adding NH₄PF₆ (4.8 g, 29.4 mmol) to a solution of [H₃TIMEN^{*t*-Bu}]Cl₃ (5.6 g, 9.7 mmol) in 20 mL of methanol. The white hexafluorophosphate salt precipitated immediately, and was collected by filtration, washed with small portions of cold methanol, and dried in a vacuum (6.7 g; yield: 76%).

¹H NMR (300 MHz, *d*₆-DMSO, 20 °C): δ = 9.19 (s, 3H), 7.99 (s, 3H), 7.66 (s, 3H), 4.14 (t, ³J(H,H) = 6.0 Hz, 6H), 2.99 (t, ³J(H,H) = 6.0 Hz, 6H), 1.57 ppm (s, 27H). ¹³C NMR (100 MHz, *d*₆-DMSO, 20 °C): δ = 134.3, 122.7, 122.0, 59.6, 52.1, 46.0, 29.0 ppm. Anal. Calcd for C₂₇H₄₈F₁₈N₇P₃: C, 35.81; H, 5.34; N, 10.83. Found: C, 35.48; H, 5.02; N, 10.90.

[TIMEN^{Bz}](PF₆)₃ (**H₃5c**). A 50 mL flask was charged with tris(2-chloroethyl)amine (9.85 g, 48.2 mmol) and *N*-benzylimidazole (22.9 g, 144.8 mmol), and the mixture was heated to 150 °C for 2 days, during which a brown solid formed. The solid was isolated and dissolved in 100 mL of methanol, and the filtered solution was evaporated to dryness to yield the crude product [H₃TIMEN^{Bz}]Cl₃ (32 g; yield: 98%). The hygroscopic chloride salt was converted to stable [H₃TIMEN^{Bz}](PF₆)₃ by adding NH₄PF₆ (22.6 g, 29.4 mmol) to a solution of [H₃TIMEN^{Bz}]Cl₃ (32 g, 47.1 mmol) in 50 mL of methanol. The white hexafluorophosphate salt precipitated immediately, and was collected by filtration, washed with small portions of cold methanol, and dried in a vacuum (39.6 g; yield: 81%).

¹H NMR (300 MHz, *d*₆-DMSO, 20 °C): δ = 9.20 (s, 3H), 7.76 (s, 3H), 7.63 (s, 3H), 7.37 (m, 15H), 5.41 (s, 6H), 4.13 (t, ³J(H,H) = 6.0 Hz, 6H), 2.93 (t, ³J(H,H) = 6.0 Hz, 6H). ¹³C NMR (100 MHz, *d*₆-DMSO, 20 °C): δ = 136.0, 134.5, 128.8, 128.6, 128.1, 122.8, 122.1, 52.0, 51.8, 46.2 ppm. Anal. Calcd for C₃₆H₄₂F₁₈N₇P₃: C, 42.91; H, 4.20; N, 9.73. Found: C, 43.30; H, 4.19; N, 9.87.

[TIMEN^{*t*-Bu}](**5b**). A solution of potassium *tert*-butoxide (0.15 g, 1.35 mmol) in THF was added dropwise to a suspension of **H₃5b** (0.41 g, 0.45 mmol) in 5 mL of THF. A clear colorless solution was formed upon addition of the base. The solution was evaporated to dryness, and the white residue was dissolved in 15 mL of diethyl ether. The resulting solution was filtered, and the filtrate was evaporated to dryness in a vacuum. The white solid was collected, washed with cold pentane, and dried in a vacuum (0.15 g; yield: 71%).

¹H NMR (400 MHz, *d*₆-benzene, 20 °C): δ = 6.67 (d, ³J(H,H) = 2.0 Hz, 3H), 6.42 (d, ³J(H,H) = 2.0 Hz, 3H), 3.84 (t, ³J(H,H) = 6.0 Hz, 6H), 2.71 (t, ³J(H,H) = 6.0 Hz, 6H), 1.49 (s, 27H). ¹³C NMR (100 MHz, *d*₆-benzene, 20 °C): δ = 213.6, 119.9, 115.3, 57.5, 56.3, 50.5, 32.1 ppm. Anal. Calcd for C₂₇H₄₅N₇: C, 69.34; H, 9.70; N, 20.96. Found: C, 69.28; H, 9.71; N, 21.08.

[TIMEN^{Bz}](**5c**). A solution of potassium *tert*-butoxide (0.14 g, 1.2 mmol) in THF was added dropwise to a suspension of **H₃5c** (0.40 g, 0.4 mmol) in 5 mL of THF. A clear colorless solution was formed upon addition of the base. The solution was evaporated to dryness,

(37) Neese, F. *QCPE Bull.* **1995**, *15*, 5.

(38) O'Connor, C. J. *Prog. Inorg. Chem.* **1982**, *29*, 203–283.

(39) Arduengo, A. J.; Gentry, F. P.; Taverkerc, P. K.; Simmons, H. E. U.S. Patent 6177575, 2001.

(40) Ward, K. J. *Am. Chem. Soc.* **1935**, *57*, 914–916.

(41) Kubas, G. J. *Inorg. Synth.* **1979**, *19*, 90–92.

and the white residue was dissolved in 15 mL of diethyl ether. The resulting solution was filtered, and the filtrate was evaporated to yield a slightly yellow oily compound (0.16 g; yield: 70%).

^1H NMR (400 MHz, d_6 -benzene, 20 °C): δ = 7.1 (m, 15H), 6.49 (d, $^3J(\text{H,H})$ = 2.0 Hz, 3H), 6.22 (d, $^3J(\text{H,H})$ = 2.0 Hz, 3H), 4.99 (s, 6H), 3.86 (t, $^3J(\text{H,H})$ = 6.0 Hz, 6H), 2.71 (t, $^3J(\text{H,H})$ = 6.0 Hz, 6H). ^{13}C NMR (100 MHz, d_6 -benzene, 20 °C): δ = 211.8, 139.4, 129.1, 128.0, 121.6, 118.4, 57.3, 55.4, 50.0 ppm.

$[(\text{TIMEN}^{\text{Me}})_2\text{Ag}_3](\text{PF}_6)_3$ (**9**). **H₃5a** (0.49 g, 0.62 mmol) was dissolved in 50 mL of DMSO, and to this solution was added Ag_2O (0.22 g, 0.95 mmol). The mixture was heated to 75 °C for 12 h. The resulting suspension was filtered through Celite, and to the filtrate was added an equal amount of water to give a white powder. The solid was collected by filtration, washed with ether, and dried under vacuum (0.33 g, yield: 76%).

^1H NMR (400 MHz, d_6 -DMSO, 20 °C): δ = 7.39 (s, br, 6H), 4.09 (s, br, 6H), 3.73 (s, 9H), 2.96 ppm (s, br, 6H). ^{13}C NMR (100 MHz, d_6 -DMSO, 20 °C): δ = 179.4, 122.7, 121.9, 54.1, 48.5, 38.1 ppm. Anal. Calcd for $\text{C}_{36}\text{H}_{54}\text{N}_{14}\text{Ag}_3\text{P}_3\text{F}_{18}\cdot 3\text{DMSO}$: C, 30.10; H, 4.33; N, 11.70. Found: C, 28.71; H, 4.18; N, 11.62.

$[(\text{TIMEN}^{\text{Me}})_2\text{Cu}_3](\text{PF}_6)_3$ (**10**). A solution of copper(I) bromide (56 mg, 0.40 mmol) in 2 mL of acetonitrile was added dropwise to a solution of **9** (190 mg, 0.13 mmol) in 4 mL of acetonitrile. The reaction mixture was allowed to stir for 1 h, and the resulting suspension was filtered. Addition of 10 mL of diethyl ether to the filtrate induced precipitation of a white crystalline powder. The precipitate was filtered, washed with diethyl ether, and dried in a vacuum (116 mg; yield: 68%). Colorless crystals suitable for X-ray diffraction analysis were grown by diffusion of diethyl ether into a saturated solution of **10** in acetonitrile at room temperature.

^1H NMR (300 MHz, d_3 -acetonitrile, 20 °C): δ = 6.97 (s, 3H), 6.95 (s, 3H), 3.99 (t, $^3J(\text{H,H})$ = 6.0 Hz, 6H), 3.71 (s, 9H), 2.98 ppm (t, $^3J(\text{H,H})$ = 6.0 Hz, 6H). ^{13}C NMR (100 MHz, d_3 -acetonitrile, 20 °C): δ = 178.4, 122.5, 121.9, 57.9, 48.7, 38.6 ppm. Anal. Calcd for $\text{C}_{36}\text{H}_{54}\text{N}_{14}\text{Cu}_3\text{P}_3\text{F}_{18}$: C, 33.04; H, 4.16; N, 14.99. Found: C, 32.79; H, 4.12; N, 15.08.

$[(\text{TIMEN}^{\text{t-Bu}})\text{Cu}](\text{PF}_6)$ (**11b**). A solution of tetrakis(acetonitrile)-copper(I) hexafluorophosphate (0.12 g, 0.32 mmol) in acetonitrile was added dropwise to a solution of **5b** (0.15 g, 0.32 mmol) in 3 mL of acetonitrile. The reaction mixture was stirred for 1 h, and 10 mL of diethyl ether was added to cause precipitation of **11b** as an off-white powder. The precipitate was collected by filtration, washed with diethyl ether, and dried in a vacuum (0.13 g; yield: 60%). Colorless crystals suitable for X-ray diffraction analysis were grown by diffusion of diethyl ether into a saturated solution of **11b** in THF at room temperature.

^1H NMR (400 MHz, d_3 -acetonitrile, 20 °C): δ = 7.19 (d, $^3J(\text{H,H})$ = 2.0 Hz, 3H), 6.92 (d, $^3J(\text{H,H})$ = 2.0 Hz, 3H), 3.67 (dd, $^3J(\text{H,H})$ = 14.0 Hz, $^3J(\text{H,H})$ = 4.0 Hz, 3H), 3.43 (dd, $^3J(\text{H,H})$ = 14.0 Hz, $^3J(\text{H,H})$ = 10.0 Hz, 3H), 2.90 (dd, $^3J(\text{H,H})$ = 14.0 Hz, $^3J(\text{H,H})$ = 4.0 Hz, 3H), 2.34 (dd, $^3J(\text{H,H})$ = 14.0 Hz, $^3J(\text{H,H})$ = 10.0 Hz, 3H), 1.52 (s, 27H). ^{13}C NMR (100 MHz, d_3 -acetonitrile, 20 °C): δ = 187.0, 122.3, 117.6, 60.7, 57.8, 51.0, 31.1 ppm. Anal. Calcd for $\text{C}_{27}\text{H}_{45}\text{N}_7\text{CuPF}_6$: C, 47.96; H, 6.71; N, 14.50. Found: C, 48.12; H, 6.64; N, 14.36.

$[(\text{TIMEN}^{\text{Bz}})\text{Cu}](\text{Br})$ (**11c**). A solution of copper(I) bromide (0.035 g, 0.25 mmol) in acetonitrile was added dropwise to a solution of **5c** (0.14 g, 0.25 mmol) in 3 mL of acetonitrile. The mixture was allowed to stir for 1 h, and then the solution was evaporated to dryness. The solid residue was dissolved in 10 mL of CH_2Cl_2 , and the resulting solution was filtered through Celite. Diethyl ether was added to the filtrate to cause precipitation of **11c** as a slightly yellow powder. The precipitate was collected by filtration, washed with diethyl ether, and dried under vacuum (0.1 g; yield: 56%). Colorless crystals suitable for X-ray diffraction analysis were grown by slow diethyl ether diffusion into a saturated solution of **11c** in CH_2Cl_2 at room temperature.

^1H NMR (400 MHz, d_3 -acetonitrile, 20 °C): δ = 7.09 (m, 6H), 6.95 (d, $^3J(\text{H,H})$ = 2.0 Hz, 3H), 6.83 (m, 9H), 6.76 (d, $^3J(\text{H,H})$ = 2.0

Hz, 3H), 4.97 (s, br, 6H), 3.75 (s, br, 6H), 2.72 (s, br, 6H). ^{13}C NMR (100 MHz, d_3 -acetonitrile, 20 °C): δ = 189.7, 138.6, 128.9, 127.9, 127.6, 122.0, 118.6, 58.1, 54.3, 48.5 ppm. Anal. Calcd for $\text{C}_{36}\text{H}_{39}\text{N}_7\text{CuBr}$: C, 60.60; H, 5.51; N, 13.75. Found: C, 60.45; H, 5.58; N, 13.71.

$[(\text{TIMEN}^{\text{Bz}})\text{Cu}](\text{SO}_3\text{CF}_3)_2$ (**12**). Method A: A solution of silver triflate (0.072 g, 0.28 mmol) in acetonitrile was added dropwise to a solution of **11c** (0.1 g, 0.14 mmol) in 5 mL of acetonitrile. A black precipitate of Ag^0 formed upon addition of the silver salt. The mixture was filtered through Celite, and the filtrate was evaporated to dryness. The brown solid residue was collected by filtration, washed with diethyl ether, and dried under vacuum (0.052 g; yield: 40%). Method B: A solution of copper(II) triflate (0.114 g, 0.31 mmol) in benzene was added dropwise to a solution of **5c** (0.18 g, 0.31 mmol) in 10 mL of benzene. The reaction mixture was stirred for 1 h, during which a brown-black precipitate formed. The precipitate was collected by filtration, washed with diethyl ether, and dried in a vacuum (0.19 g; yield: 66%).

Anal. Calcd for $\text{C}_{38}\text{H}_{39}\text{N}_7\text{CuO}_6\text{S}_2\text{F}_6$: C, 49.00; H, 4.22; N, 10.53. Found: C, 48.78; H, 4.20; N, 10.62.

Crystallographic Details for $[(\text{TIMEN}^{\text{Me}})_2\text{Cu}_3](\text{PF}_6)_3\cdot 2.5\text{CH}_3\text{CN}$ (10**).** A crystal of dimensions $0.17 \times 0.13 \times 0.05 \text{ mm}^3$ was mounted on a glass fiber. A total of 24 440 reflections ($-15 \leq h \leq 14$, $-15 \leq k \leq 15$, $-27 \leq l \leq 27$) were collected at $T = 100(2) \text{ K}$ in the range from 1.75° to 27.51° , of which 12 496 were unique ($R_{\text{int}} = 0.0381$); Mo K α radiation ($\lambda = 0.71073 \text{ \AA}$). The structure was solved by direct methods (Shelxtl Version 6.10, Bruker AXS, Inc., 2000). All non-hydrogen atoms were refined anisotropically. Hydrogen atoms were placed in calculated idealized positions. The residual peak and hole of electron densities were 1.44 and -1.27 e \AA^{-3} . Three sites occupied by acetonitrile were identified in the asymmetric unit. Two were ordered and fully occupied. A third site was considerably disordered and was treated by SQUEEZE as a diffuse contribution. In the resulting void space, a contribution of 20 e^- per unit cell was found and taken to represent 0.5 molecules for each Cu_3 complex, giving a total of $2.5\text{CH}_3\text{CN}$ in the asymmetric unit. The absorption coefficient was 1.329 mm^{-1} . The least squares refinement converged with residuals of $R(F) = 0.059$, $wR(F^2) = 0.1615$, and a GOF = 0.983 ($I > 2\sigma(I)$). $\text{C}_{36}\text{H}_{54}\text{N}_{14}\text{Cu}_3\text{P}_3\text{F}_{18}\cdot 2.5\text{CH}_3\text{CN}$, space group $P-1$, triclinic, $a = 11.6256(18)$, $b = 12.2828(19)$, $c = 21.027(3)$, $\alpha = 89.234(3)^\circ$, $\beta = 78.523(3)^\circ$, $\gamma = 71.615(2)^\circ$, $V = 2788.4(8) \text{ \AA}^3$, $Z = 2$, $\rho_{\text{calcd}} = 1.681 \text{ Mg/m}^3$.

Crystallographic Details for $[(\text{TIMEN}^{\text{t-Bu}})\text{Cu}](\text{PF}_6)$ (11b**).** A crystal of dimensions $0.49 \times 0.22 \times 0.04 \text{ mm}^3$ was mounted on a glass fiber. A total of 8778 reflections ($-10 \leq h \leq 10$, $-12 \leq k \leq 12$, $-15 \leq l \leq 15$) were collected at $T = 100(2) \text{ K}$ in the range from 1.48° to 22.50° , of which 4093 were unique ($R_{\text{int}} = 0.0317$); Mo K α radiation ($\lambda = 0.71073 \text{ \AA}$). The structure was solved by direct methods (Shelxtl Version 6.10, Bruker AXS, Inc., 2000). All non-hydrogen atoms were refined anisotropically. Hydrogen atoms were placed in calculated idealized positions. The residual peak and hole electron of densities were 0.543 and $-0.430 \text{ e \AA}^{-3}$. The absorption coefficient was 0.812 mm^{-1} . The least squares refinement converged normally with residuals of $R(F) = 0.0346$, $wR(F^2) = 0.0811$, and a GOF = 0.967 ($I > 2\sigma(I)$). $\text{C}_{27}\text{H}_{45}\text{N}_7\text{CuPF}_6$, space group $P-1$, triclinic, $a = 9.586(4)$, $b = 11.901(4)$, $c = 14.205(5)$, $\alpha = 95.194(6)^\circ$, $\beta = 102.968(6)^\circ$, $\gamma = 92.142(6)^\circ$, $V = 1539.9(6) \text{ \AA}^3$, $Z = 2$, $\rho_{\text{calcd}} = 1.431 \text{ Mg/m}^3$.

Crystallographic Details for $[(\text{TIMEN}^{\text{Bz}})\text{Cu}]\text{Br}$ (11c**).** A crystal of dimensions $0.26 \times 0.18 \times 0.05 \text{ mm}^3$ was mounted on a glass fiber. A total of 29 736 reflections ($-15 \leq h \leq 15$, $-21 \leq k \leq 21$, $-22 \leq l \leq 22$) were collected at $T = 100(2) \text{ K}$ in the range from 1.13° to 22.50° , of which 13 209 were unique ($R_{\text{int}} = 0.0387$); Mo K α radiation ($\lambda = 0.71073 \text{ \AA}$). The structure was solved by direct methods (Shelxtl Version 6.10, Bruker AXS, Inc., 2000). All non-hydrogen atoms were refined anisotropically. Hydrogen atoms were placed in calculated idealized positions. The residual peak and hole electron of densities were 0.469 and $-0.554 \text{ e \AA}^{-3}$. The absorption coefficient was 1.876 mm^{-1} . The least squares refinement converged normally with residuals

of $R(F) = 0.0428$, $wR(F^2) = 0.0869$, and a GOF = 0.932 ($I > 2\sigma(I)$). $C_{36}H_{39}N_7CuBr$, space group $P-1$, triclinic, $a = 14.131(4)$, $b = 20.193(6)$, $c = 20.73(6)$, $\alpha = 116.583(5)^\circ$, $\beta = 98.521(5)^\circ$, $\gamma = 98.871(5)^\circ$, $V = 5063(2) \text{ \AA}^3$, $Z = 6$, $\rho_{\text{calcd}} = 1.404 \text{ Mg/m}^3$.

Acknowledgment. This work was supported by the University of California, San Diego. We thank Dr. Peter Gantzel and Prof. Arnold L. Rheingold for help with the crystallography.

Supporting Information Available: Cyclic voltammogram of complexes **11b** and **11c**, a set of molecular orbitals of calculated compound $[\text{TIMEN}^{\text{Me}}\text{Cu}]^{2+}$, and complete crystallographic details of the X-ray structures of **10**, **11b**, and **11c** (CIF and PDF). This material is available free of charge via the Internet at <http://pubs.acs.org>.

JA036880+